Journal of Building Engineering 105 (2025) 112335

Contents lists available at ScienceDirect

Journal of Building Engineering

journal homepage: www.elsevier.com/locate/jobe

Valorization of municipal waste glass powder in autoclaved aerated concrete: Microstructural evolution and performance analysis

C. Straub [a,b,c], B. Yuan [a,b,*], H.J.H. Brouwers [b], W. Chen [b,a,**]

[a] State Key Lab of Silicate Materials for Architectures, Wuhan University of Technology, 430070, Wuhan, PR China
[b] Department of the Built Environment, Eindhoven University of Technology, P.O. Box 513, 5600 MB, Eindhoven, the Netherlands
[c] Materials Innovation Institute, P.O. Box 5008, 2600 GA, Delft, the Netherlands

ARTICLE INFO

Keywords:
Autoclaved aerated concrete
Municipal waste glass powder
Sustainability
Microstructure evolution
Industrial application

ABSTRACT

This study investigates the incorporation of municipal waste glass powder in autoclaved aerated concrete (AAC) through comprehensive experimental analysis and industrial-scale simulation. The experimental program encompasses characterization of raw materials, evaluation of fresh and hardened properties, and microstructural analysis. Results show that waste glass powder replacement up to 40 % enhances compressive strength and improves the A-value by 37 %, attributed to enhanced reactivity and optimized pore structure. The crystallinity of tobermorite decreases with increasing waste glass powder content, while the amorphous nature of glass powder promotes the formation of semi-crystalline calcium silicate hydrates. This work establishes practical guidelines for sustainable waste glass powder utilization in AAC production while improving material performance.

1. Introduction

Autoclaved aerated concrete (AAC) is a lightweight, precast building material that has gained popularity in the construction industry due to its excellent properties, such as low thermal conductivity, low density, low shrinkage, and good fire resistance [1,2]. The typical raw materials for producing AAC include cement, lime, gypsum, quartz, water, and metallic aluminum powder, which acts as a foaming agent [1,3]. To increase the sustainability or improve the performance, extensive research has been conducted on the replacement of raw materials in AAC with various waste products and supplementary cementitious materials (SCMs) [4–7].

Several studies have investigated the use of fly ash [8], blast furnace slag [4], rice husk ash [5], copper tailings [9], and municipal solid waste incineration bottom ash [10,11] as replacements for quartz in AAC. These studies have demonstrated that incorporating these waste materials can lead to improvements in the mechanical and thermal properties of AAC [12]. The authors attributed these improvements to various factors, such as the pozzolanic reaction of the waste materials, their contribution to the formation of tobermorite, and the refinement of the pore structure [13,14].

One promising waste stream for AAC production is municipal waste glass powder [6,15]. During the recycling process of municipal

* Corresponding author. State Key Lab of Silicate Materials for Architectures, Wuhan University of Technology, 430070, Wuhan, PR China.
** Corresponding author. Department of the Built Environment, Eindhoven University of Technology, P.O. Box 513, 5600 MB, Eindhoven, the Netherlands.
E-mail addresses: yuan.bo@whut.edu.cn (B. Yuan), chen.wei@whut.edu.cn (W. Chen).

https://doi.org/10.1016/j.jobe.2025.112335
Received 25 September 2024; Received in revised form 24 January 2025; Accepted 10 March 2025
Available online 11 March 2025

Table 1
Chemical compositions of the raw materials (wt.%).

Chemical compositions	Quartz	Anhydrite	Cement	Portlandite	Lime	Waste glass
$Na_2O + K_2O$	–	0.46	1.18	0.03	0.17	12.70
MgO	–	1.80	1.40	0.51	0.82	1.50
Al_2O_3	0.14	0.56	5.60	0.20	0.64	2.10
SiO_2	99.5	2.10	20.60	0.48	1.20	69.70
SO_3	0.01	41.90	5.00	0.07	0.05	0.14
CaO	–	38.50	63.10	70.60	94.40	10.80
Fe_2O_3	0.03	0.19	2.10	0.21	0.03	0.55
L.O.I.	0.14	3.08	2.00	27.40	2.50	3.20
Specific density [g/cm^3]	2.65	2.95	3.12	2.31	3.24	2.50
Blaine surface are [cm^2/g]	6070	–	3520	–	4270	1430

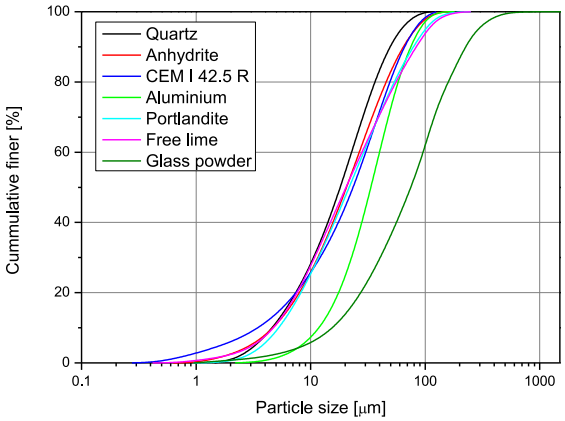

Fig. 1. Particle size distribution of raw materials.

waste glass, a certain fraction of material is obtained which is not suitable for recycling due to its small particle size. This fraction also contains a high amount of contaminants, such as food remains and label residues. The chemical composition of this waste glass powder is similar to that of bottle glass, with 70 % SiO_2, 12 % CaO, and 12 % Na_2O, along with minor elements [16,17]. The glass powder has a slightly coarser particle size distribution compared to typical cement powder, with 90 % of the glass particles passing through a 200 µm sieve.

The utilization of municipal waste glass in construction materials has also been the subject of numerous studies in recent years [6, 17,18]. Researchers have investigated the use of waste glass as a partial replacement for cement in concrete and as a supplementary cementitious material in various applications [19,20]. These studies have highlighted the potential benefits of using waste glass, such as reducing the consumption of natural resources, decreasing the amount of waste sent to landfills, and improving the mechanical and durability properties of the final products.

Despite these initial findings on waste glass incorporation in construction materials, the application of waste glass powder in AAC production has not been extensively explored. The existing studies [6,7,18] have mainly focused on mechanical properties and basic feasibility assessment. Previous research has reported improvements in compressive strength when using waste glass as a partial replacement for quartz in AAC [6]. Similar findings have been demonstrated in autoclaved sand-lime products [7]. Additionally, the successful synthesis of Al-substituted 11 Å tobermorite using waste glass cullet as a precursor has been reported [18]. However, a comprehensive understanding of the effects of waste glass powder on AAC properties, particularly the microstructural evolution and reaction mechanisms during the autoclaving process, is still lacking.

It is worth noting that most existing studies on AAC have focused on performance evaluation, and few have been able to directly simulate the industrial production process due to limitations in experimental equipment and facilities. This gap between laboratory research and practical application makes it challenging to translate research findings into actionable guidelines for industrial production [21,22]. To bridge this gap, the present study has established a comprehensive experimental setup that closely mimics the industrial production process of AAC. The research encompasses the entire process, including sample molding, preparation, autoclaving, testing, and characterization. By adopting this holistic approach, the study not only investigates the feasibility of replacing quartz with waste glass from a theoretical perspective but also examines the implications of this substitution from an industrial production standpoint.

This study aims to address these research gaps by conducting a comprehensive investigation of the effects of municipal waste glass powder on the properties of AAC when used as a replacement for quartz. The experimental program includes the characterization of

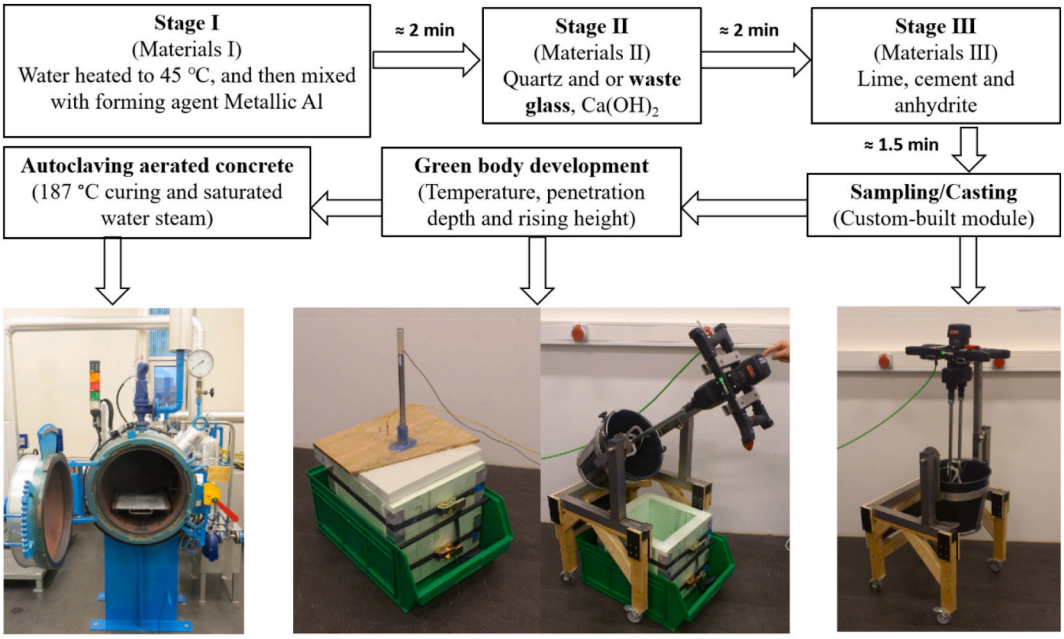

Recipes	substration level	Quartz	Glass	Lime	Cement	Portlandite	Anhydrite	Aluminium	Water	W/P
Reference		8.0	0	1	2.4	0.3	0.3	0.01	7.50	0.625
V1	Glas 8%	7.4	0.66*						7.50	0.625
V2	Glas 5 %	7.6	0.42*						7.50	0.625
V3	Glas 10 %	7.2	0.82*						7.50	0.625
V4		7.2	1.15**						7.50	0.625
V5		7.2	0.82						6.90	0.575
V6		7.2	0.80***						7.50	0.625
V7	Glas 20 %	6.4	1.65						6.30	0.525
V8	Glas 40 %	4.8	3.30						7.10	0.592
V9	Glas 60 %	3.2	4.95						6.46	0.538

Fig. 2. Mixing procedure and recipes of the prepared autoclaved aerated concrete with different replacing levels of municipal waste glass powder (Notes: the total weight of solids is 12 kg; *with moisture content; ** calculated replacement by SiO_2-content, other compounds neglected; *** glass powder washed and dried).

raw materials, evaluation of fresh and hardened state properties, microstructure, and reaction products of AAC containing municipal waste glass powder. The results will be compared with a reference AAC mixture to assess the feasibility and optimal application of this waste material in AAC production. The unique aspect of this study lies in its focus on simulating the industrial production process, which sets it apart from most existing research on AAC. By closely replicating the entire production process, from sample molding to autoclaving and characterization, this study aims to provide practical insights and guidelines that can be directly applied to industrial-scale AAC production.

2. Materials and experiment

2.1. Materials

The sand-based reference recipe for the experiments was obtained from HESS AAC Systems. X-ray Fluorescence (XRF) with pressed powder tablets using a PANalytical Epsilon 3 instrument was employed to determine the chemical compositions of the raw materials. A Malvern Mastersizer 2000 laser granulometer was used to measure the particle size distributions. The results are presented in Table 1 and Fig. 1, respectively.

2.2. Sample preparation

The preparation of the AAC samples involved several steps, as shown in Fig. 2. First, the required amou nt of water, calculated based on the water-to-powder (W/P) ratio, was heated to 45 °C and added to a mixer (Swinko EZR 22 R,R/L with a 4-bladed propeller mixing

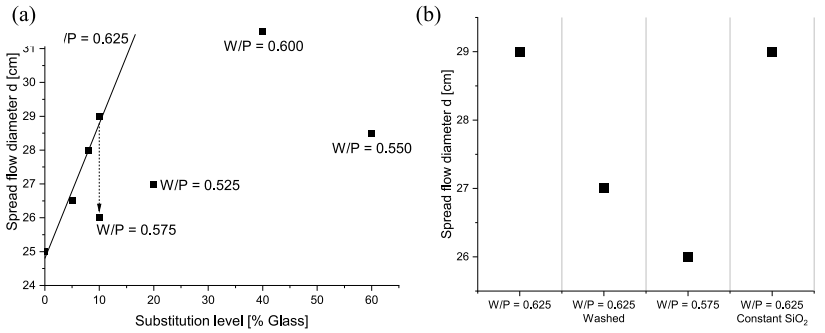

Fig. 3. (a) Spread flow of prepared AAC with different substitution levels of municipal waste glass powder and water to powder ratios (W/P) and (b) the effect of contaminants in waste glass powder (10 % substitution level) on the flowability.

rod), stirring at a low speed. Concurrently, the aluminium powder was manually pre-dispersed in water in a separate container. Secondly, quartz or waste glass and portlandite were added to the mixer sequentially and mixed for at least 60 s to ensure a homogeneous mixture. Lime was then introduced at time = 0, followed by cement and anhydrite after 30 s. Mixing was continued for an additional 90 s before the pre-dispersed aluminium powder suspension was finally added to the mixer.

After casting, the samples were allowed to set for approximately 12 h to gain the initial strength before being demoulded. The demoulded samples were immediately transferred to an autoclave (Maschinenbau Scholz GmbH & Co. KG/steam generator: WIMA ED36) for curing. The autoclaving process followed a specific sequence: 20 min of vacuum (−0.8 bar), heating to 187 °C/11 bar over 1.5 h, maintaining a plateau at 187 °C/11 bar for 5 h, and cooling to 20 °C/0 bar within 1.5 h. Following the autoclaving process, a band saw was used to remove at least 5 cm from each side of the sample. This step was performed to obtain an undisturbed core structure, minimizing the influence of the "wall-effect" and ensuring that the samples were representative of the bulk material properties.

2.3. Test methods

2.3.1. Green body development

After mixing, the spread flow of the mix was evaluated using a cone test (diameter: 7 cm, height: 6 cm, volume: 244 ml). The cone was filled with the mixture, and then vertically lifted. The diameter of the resulting cake on the glass plate was measured and recorded. Meanwhile, the slurry was poured into insulated moulds (XPS with parting agent, 27 l in volume, semi-calorimetric environment). A data logger was used to record the temperature and rising behavior of the mixture, as depicted in Fig. 2.

The stiffening of the mix was assessed using a specialized indenter (pointy cone, mass: 30 g) placed vertically on the surface of the mass. The cone penetrates the mass under its own weight, and the penetration depth over time serves as an indicator of the mix's stiffness, similar to the Vicat needle setup for determining setting time. The measurement is terminated when the penetration depth reaches less than 20 mm.

2.3.2. Hardened state analysis

The prepared AAC material was cut into cubes (100 × 100 × 100 mm^3) for raw density (or apparent density) and compressive strength measurements. The cubes were polished and oven-dried (60 °C, forced ventilation) until reaching a constant weight. After cooling to room temperature, the raw density and compressive strength were determined using a testing machine (FORM + TEST Seidner + Co. GmbH, MEGA 110–200 D-S). This approach is comparable to the EN 771-4 and EN 771 standards. The total porosity (Φ_{total}) of AAC samples was determined as the difference between total porosity and air porosity, using the Equation $\Phi_{total} = (1 - \rho_{raw}/\rho_{true}) \times 100$ %, where ρ_{raw} is the raw density and ρ_{true} is the true density of the sample.

The thermal conductivity of the samples was measured using an ISOMET model 2104 device (Applied Precision) by taking multiple measurements on a polished surface. Scanning Electron Microscopy (SEM) using a FEI Quanta 600 was employed for microscopic analysis of the powders. Pictures were taken under high vacuum ($<1.3 \bullet 10^{-4}$ mbar) without conductive coating with an acceleration voltage of 10 kV. The phase composition was investigated using X-Ray Diffractometry (XRD) with a PANalytical X'Pert PRO MPD equipped with CuKα radiation and an X'Celerator RTMS detector. The XRD measurements were performed using back loading preparation, a 20 mm sample diameter, 15 mm irradiated sample length, 5–90 °2θ range, 0.02 °2θ/step, 41.3 s/step, variable slits, 40 mA, and 45 kV.

Following the RILEM AAC5.2 standard, the samples were immersed in water for 72 h for saturation, and the initial length was measured within 30 min after removal from the water. The drying shrinkage and mass of the samples were monitored while the samples were stored in a chamber maintained at 20 ± 2 °C and 43 ± 2 % humidity (controlled by K_2CO_3-ss). Once the samples reached a constant length, they were oven-dried at 105 °C until achieving constant masses, and the moisture contents of individual samples were determined.

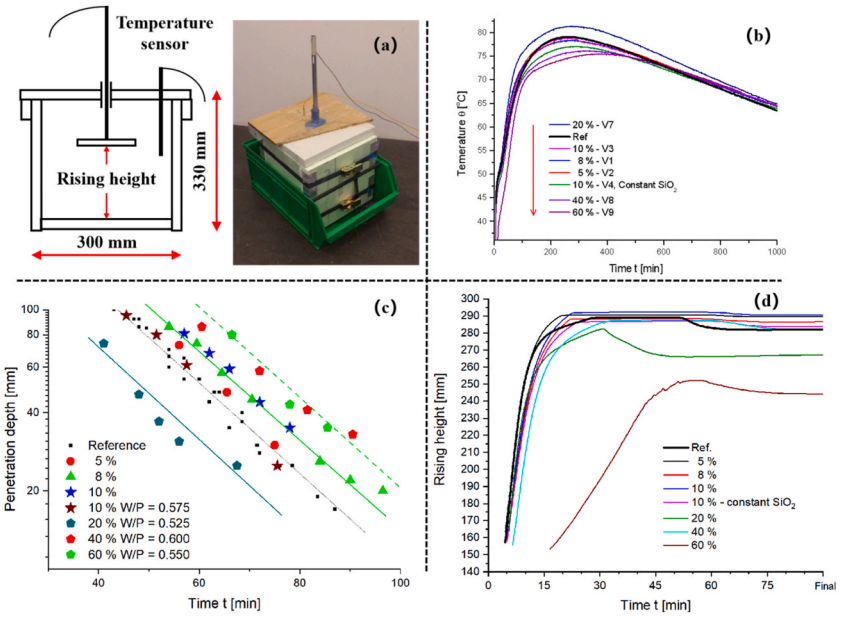

Fig. 4. Autoclaved aerated concrete with different replacing levels of municipal waste glass powder: (a) temperature versus time; (b) penetration depth and (c) rising height of green body.

3. Results

3.1. Municipal waste glass powder on the workability of AAC

The influence of municipal waste glass powder (GP) content on the spread flow of AAC slurry at various water-to-powder (W/P) ratios is presented in Fig. 3a. The linear portion of the curves represents the change in flowability with increasing GP content at a constant W/P ratio. It is evident that the incorporation of GP significantly increases the flowability of the slurry, e.g. the spread flow diameter of samples increases from 25 cm (reference) to approximately 29 cm when 10 % of quartz is replaced by GP. GP consists primarily of SiO_2 (69.7 wt%), CaO (10.8 wt%), and alkali oxides ($Na_2O + K_2O$, 12.7 wt%), with a specific density of 2500 kg/m^3. Although the alkali content in the glass is not readily soluble, the low Blaine surface area of the glass powder contributes to the improved flowability of the AAC slurry.

Moreover, the relatively high loss on ignition (LOI) value of 3.2 wt% in GP, which suggests the presence of contaminants in GP, plays a significant role in improving the flowability of the AAC slurry. As shown in Fig. 3a, the spread flow diameter of the mixture containing washed GP is lower than that of the unwashed GP at the same W/P ratio of 0.625. This indicates that the contaminants present in GP can enhance the flowability of the slurry, possibly by acting as a plasticizing agent or reducing the water demand of the mixture. The contaminants, e.g. organic compounds, may adsorb onto the surface of the glass powder particles [23,24], altering their surface properties and reducing the attractive forces between them, thus facilitating a better dispersion and improved flowability.

To further investigate the effect of contaminants on the flowability of AAC slurry, a comparison was made between mixtures containing unwashed GP, washed GP, and constant SiO_2 content at a W/P ratio of 0.625. The results (Fig. 3b) reveal that the mixture with unwashed GP exhibits the highest spread flow diameter, followed by the mixture with constant SiO_2 content, and finally the mixture with washed GP. This confirms that the contaminants present in GP plays a significant role in improving the flowability of the slurry, even when compared to a mixture with the same SiO_2 content.

Despite the increase in flowability, it is important to maintain the spread flow diameter within an acceptable range (25 $\pm$ 3 cm, as determined by our previous study [25]) to ensure proper mixing, casting, and rising of the AAC. As shown in Fig. 3a, the flowability of the slurry remains within this range for GP substitution levels up to 60 % at the investigated W/P ratios.

3.2. Green body development

Fig. 4a presents the setup of measuring the temperature, penetration depth, and rising height of AAC samples containing different levels of GP. These parameters provide valuable insights into the hydration kinetics, setting behavior, and pore structure development of the AAC green body. As shown in Fig. 4b, the temperature evolution of the AAC mixtures is notably affected by the GP content. With increasing GP substitution levels, the hydration reaction rate decreases, as evidenced by the slower temperature rise and the lower peak temperatures. The reference samples reach a maximum temperature of approximately 78 °C, while the sample containing 60 % GP exhibits a significantly lower peak temperature of around 72 °C. Previous research has demonstrated that organic components can affect hydration kinetics of cementitious materials [23,24]. This reduction in heat release can be primarily attributed to the presence of

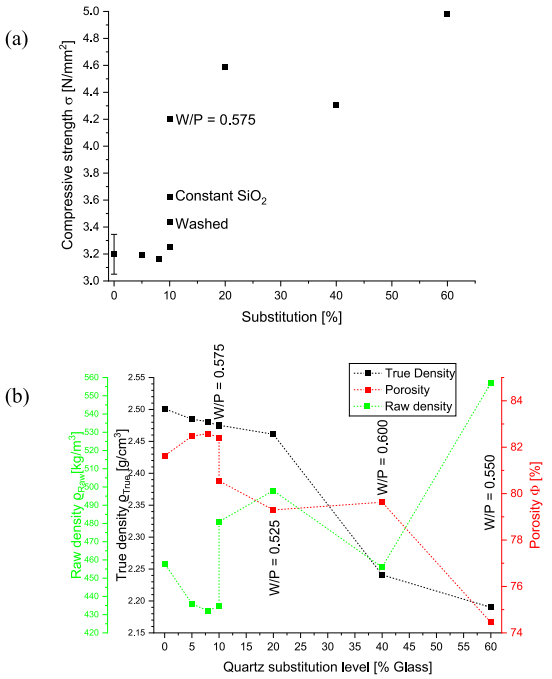

Fig. 5. Autoclaved aerated concrete with different replacing levels of municipal waste glass powder: (a) compressive strength, and (b) raw density [green], true density [black] and porosity [red].

contaminants in GP, which may hinder the hydration process through the interaction between water-soluble contaminants (primarily consisting of sugars, starch, and cellulose fibers from food and label residues) and cement particles.

The slower hydration kinetics and reduced heat release associated with increasing GP content have a direct impact on the setting behavior of the AAC green body. Fig. 4c illustrates the penetration depth over time for the different mixtures. The reference samples achieve a penetration depth of 20 mm, indicating the onset of setting, at approximately 50 min. In contrast, the samples containing GP exhibit delayed setting times, with the 60 % GP sample reaching the same penetration depth after more than 100 min.

The delayed setting and slower hydration kinetics also influence the pore structure development of the AAC green body, as depicted by the rising height curves in Fig. 4d. The reference samples exhibit a rapid increase in rising height, reaching the maximum detectable height of the equipment (284 mm) within 30 min. However, the samples containing GP show a more gradual increase in rising height, with the 60 % GP sample requiring more than 60 min to not even reach the same level. This slower pore structure development can be attributed to the delayed formation of the solid matrix, which are essential for stabilizing the porous structure.

It worth noting that the rising height curves of the samples containing GP display a characteristic shape: a steep increase, followed by a slower increase reaching a maximum and followed by a sudden drop, particularly evident in the 40 % and 60 % GP samples, arriving on a plateau. This phenomenon indicates a collapse or shrinkage of the pore structure at the detection height, which can be attributed to the insufficient strength development of the green body due to the delayed hydration and setting. The collapse of the pore structure can lead to inhomogeneities and defects in the final AAC product, compromising its quality and mechanical properties. The experimental results also demonstrate the influence of water-to-powder ratio on the green body properties of AAC containing GP. As shown in Fig. 4c, the 10 % GP sample with a reduced W/P ratio of 0.575 (brown stars) exhibits a stiffening profile similar to that of the reference sample, indicating that adjusting the W/P ratio can help to compensate for the decreased water demand and maintain the desired pore structure development.

The comparative study involving the 10 % GP sample with constant SiO_2 content and the washed 10 % GP sample further highlights the role of contaminants in the hydration and setting processes. The washed GP sample shows a temperature evolution and penetration depth profile closer to that of the reference sample. On the other hand, the sample with substitution by constant SiO_2-content exhibits a slower temperature rise and delayed setting compared to the washed GP sample and the ordinary 10 % substitution by weight. These observations confirm that the contaminants in GP is primarily responsible for the retarding effect on the hydration reaction and the prolonged setting time.

The incorporation of municipal waste glass powder in AAC production significantly influences the green body properties of the mixture. The slower hydration kinetics, reduced heat release, and delayed setting associated with increasing GP content can be primarily attributed to the presence of contaminants in GP, which hinders the hydration process. These effects lead to a prolonged pore structure development and potential issues with the stability of the green body.

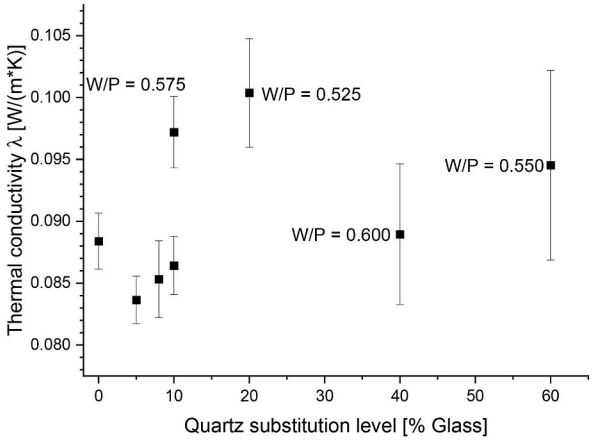

Fig. 6. Thermal conductivity of autoclaved aerated concrete with different replacing levels of municipal waste glass powder.

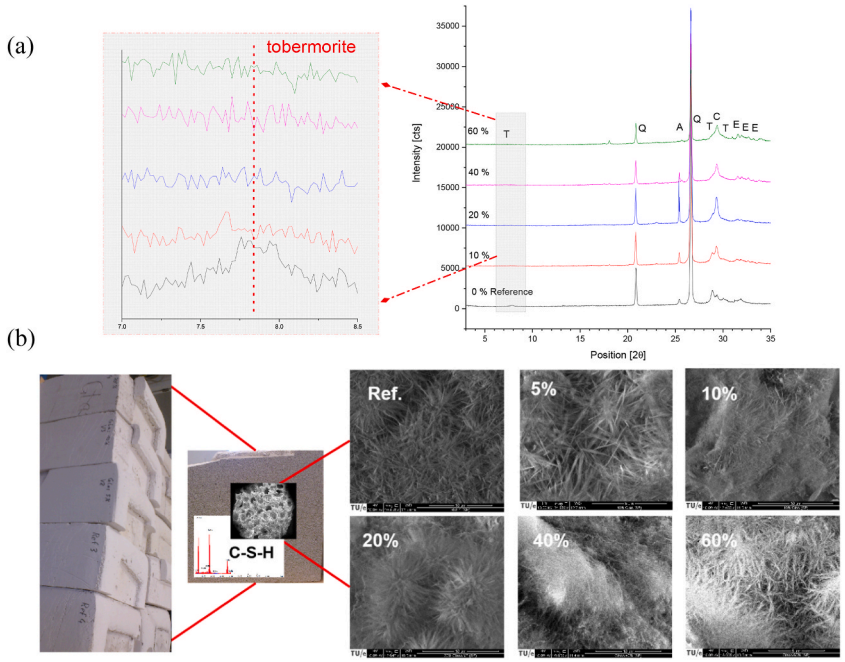

Fig. 7. Autoclaved aerated concrete with different replacing levels of municipal waste glass powder: (a) phase compositions and (b) microstructure.

3.3. Mechanical performance and pore structure of hardened samples

Fig. 5 illustrates the effects of GP content on the compressive strength and porosity of AAC. At GP contents below 10 % (Fig. 5a), the compressive strength is only marginally affected. Although washing GP to remove contaminants increases compressive strength from 3.2 MPa to 3.45 MPa, this process significantly raises production costs in industrial applications. Alternatively, reducing the water-to-powder (W/P) ratio to 0.575 enhances compressive strength to 4.2 MPa, highlighting the crucial roles of both contaminants in GP and W/P ratio adjustments in determining AAC mechanical properties at low GP levels. When GP content exceeds 10 %, a significant improvement in compressive strength is observed, with the sample containing 60 % GP achieving a remarkable 4.9 MPa, surpassing the reference sample. This enhancement can be attributed to the higher reactivity of amorphous GP compared to quartz powder under autoclaving conditions, as well as the denser and less porous microstructure formed at higher GP levels.

Fig. 5b depicts the influence of GP content on the raw density, true density, and porosity of AAC. At GP substitution levels below 10 %, the true density and porosity remain relatively unchanged compared to the reference sample. However, when the GP content surpasses 10 %, a notable decrease in both true density and porosity is observed. This trend is consistent with the compressive strength results, suggesting that the incorporation of higher levels of GP leads to a denser and less porous microstructure, which contributes to the improved mechanical performance.

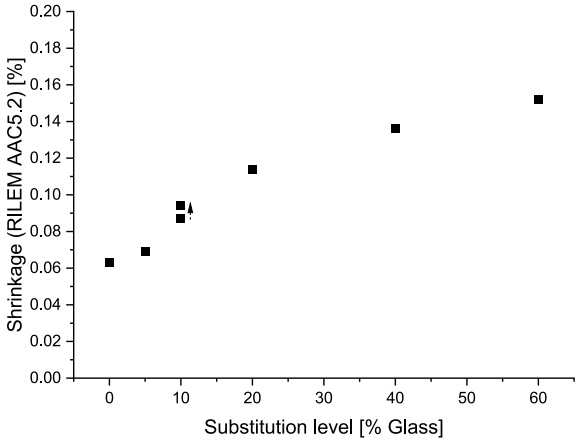

Fig. 8. Shrinkage of autoclaved aerated concrete with different replacing levels of municipal waste glass powder.

The thermal conductivity of AAC is closely related to the GP substitution level and the W/P ratio, as shown in Fig. 6. At GP contents below 10 %, the thermal conductivity is lower than that of the reference sample, indicating improved thermal insulation properties. Conversely, when the GP content exceeds 10 %, the thermal conductivity surpasses that of the reference sample. This behavior can be attributed to the changes in the porosity and pore structure of AAC induced by the incorporation of GP. The porosity and pore size distribution are the dominant factors governing the thermal conductivity of AAC, with lower porosity and smaller pore sizes generally resulting in higher thermal conductivity.

The compressive strength of AAC is closely related to the GP substitution level, the presence of contaminants, and the adjustment of the W/P ratio. The enhanced mechanical properties at higher GP contents can be attributed to the increased reactivity of the waste glass powder and the pore structure resulting from the controlled hydration and setting processes. The porosity and thermal conductivity of AAC are also influenced by the GP content, with higher substitution levels leading to reduced porosity and increased thermal conductivity. By understanding these relationships and optimizing the mixture design, it is possible to produce AAC with improved mechanical properties and tailored thermal insulation characteristics.

4. Discussion

4.1. Role of waste glass on the phase composition

The phase composition analysis provides fundamental insights into the mechanical performance and dimensional stability observed in Section 3. As shown in Fig. 7a, the intensity of the characteristic tobermorite peaks gradually decreases with increasing municipal waste glass powder content, indicating a reduction in the crystallinity of tobermorite. This phenomenon is further confirmed by the SEM results, which provide valuable insights into the morphological changes of calcium silicate hydrate (C-S-H), as a function of GP content, as depicted in Fig. 7b. In the reference sample, the C-S-H phase appears predominantly as well-crystallized tobermorite, characterized by its distinct platy and lath-like morphology. However, as the GP content increases, a gradual transition from crystalline tobermorite to amorphous C-S-H is observed. At lower GP replacement levels (e.g., 5 %, 10 % and 20 %), the C-S-H phase still exhibits some degree of crystallinity, with the presence of both tobermorite plates and amorphous regions. With further increase in GP content (e.g., 40 % and 60 %), the amorphous nature of C-S-H becomes more prominent, characterized by the absence of well-defined tobermorite crystals and the presence of a more homogeneous and gel-like morphology.

Tobermorite plays a vital role in determining the mechanical properties, dimensional stability, and durability of AAC product. The decrease in tobermorite crystallinity observed in AAC containing waste glass powder can be attributed to the unique characteristics of waste glass powder, e.g. high specific surface area, and rapid reactivity compared to quartz. The nature of waste glass powder leads to a higher dissolution rate under the hydrothermal conditions of autoclaving, resulting in an increased concentration of silica and alkali ions in the pore solution [6,7]. This altered chemical environment may hinder the formation of well-crystallized tobermorite and instead promote the development of poorly crystalline or amorphous calcium silicate hydrate (C-S-H) phases.

The impact of waste glass powder on the shrinkage behavior of AAC was evaluated using the RILEM AAC5.2 testing method (Fig. 8). The results reveal that the drying shrinkage of AAC increases with increasing waste glass powder content, ranging from 0.06 % for the reference sample to 0.15 % for the sample with 60 % waste glass powder replacement. This increase in shrinkage can be attributed to the changes in the pore structure and decreased crystallinity of tobermorite in AAC induced by the incorporation of waste glass powder. The high soloubility of waste glass powder lead to a more refined pore structure in AAC, with a higher proportion of small pores and increased pore surface area. This refined pore structure may contribute to the increased shrinkage, as smaller pores are more susceptible to capillary stresses during drying, leading to greater volumetric changes [26]. Additionally, the reduced crystallinity of tobermorite and the potential formation of amorphous C-S-H phases in AAC containing waste glass powder also contribute to the increased shrinkage, as these phases are known to have higher water retention and shrinkage potential compared to well-crystallized

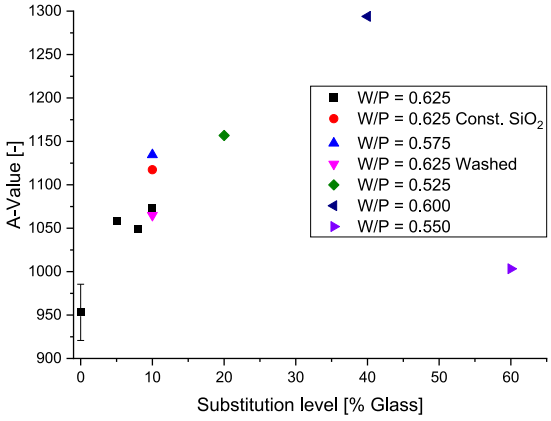

Fig. 9. A-value of samples with different replacing levels of municipal waste glass powder and water-to-powder ratios.

tobermorite.

The relationship between tobermorite crystallinity and shrinkage in AAC has been previously reported by Alexanderson [27], who found that shrinkage decreased with increasing crystallinity, defined as the percentage of 11.3 Å tobermorite out of the total amount of calcium silicate hydrates. The presence of well-crystallized tobermorite in AAC is crucial for minimizing shrinkage, as it provides a stable and rigid framework that resists volumetric changes during drying [27]. In the present study, the higher drying shrinkage of AAC containing waste glass powder can be mainly attributed to the weakened pore structure and reduced tobermorite crystallinity, as evidenced by the XRD results.

4.2. A-value: A comprehensive performance indicator for AAC

The incorporation of waste glass powder as a partial replacement for quartz in autoclaved aerated concrete (AAC) has been shown to significantly influence various properties of the final product, including flowability, green body development, mechanical performance, pore structure, phase composition, and shrinkage behavior. To gain a deeper understanding of the role of waste glass powder in AAC, it is essential to consider not only its effect on individual properties but also its overall impact on the material performance.

The A-value was developed by YTONG company in 1978, which provides a more comprehensive assessment of the material performance [28]. The A-value takes into account the relationship between the compressive strength and raw density of AAC, and is calculated using the following equation (Eq. (1)):

$$\mathrm{A-value} = \sigma \ / \ (\mathrm{const.} \times \rho^2) \tag{1}$$

where σ is the compressive strength [N/mm^2], const. is 0.016 N/g^2, and ρ is the raw density [g/cm^3]. This original formulation was published in the aforementioned publication.

As shown in Fig. 9, the A-value of AAC increases with increasing waste glass powder content up to 40 % replacement, indicating an improvement in the overall performance of the material. At 40 % replacement, the A-value increases by 37 % compared to the reference sample. However, when the waste glass powder content reaches 60 %, the A-value decreases significantly, only slightly higher than that of the reference sample.

The increase in A-value up to 40 % waste glass powder content can be attributed to the enhanced reactivity of waste glass powder during the hydrothermal curing process, promoting the formation of a denser and more homogeneous matrix. The small particle size and high specific surface area of waste glass powder led to increased dissolution of silica and alkali ions, which contribute to the formation of strength-giving phases such as calcium silicate hydrates (C-S-H) and tobermorite.

The relationship between the mechanical properties and the microstructure of AAC containing GP can be further understood by considering the morphology and arrangement of the calcium silicate hydrate (C-S-H) phases. In a typical AAC system, the strength is derived from the interlocking of plate-like tobermorite crystals, which form a random “honeycomb” or “house of cards” structure [29]. However, the incorporation of GP in AAC leads to a transition from crystalline tobermorite to amorphous C-S-H, as evidenced by the SEM and XRD results. The increased solubility of SiO_2 from the glass powder leads to the formation of more silica chains, which generate a higher proportion of needle-like or fibrous C-S-H gel, rather than well-developed tobermorite crystals. These needle-like structures interlock to form a dense, felt-like fabric, which contributes to the enhanced strength of the AAC matrix [30]. The increased amount of C-S-H gel resulting from the incorporation of GP leads to a more compact and interconnected microstructure, compensating for the lack of crystalline tobermorite.

However, the decrease in A-value at 60 % waste glass powder content suggests that there is an optimal replacement level beyond which the beneficial effects of waste glass powder are diminishing. This decline in performance can be attributed to the reduced crystallinity of tobermorite and the potential formation of amorphous C-S-H phases at higher waste glass powder contents (Fig. 7). The

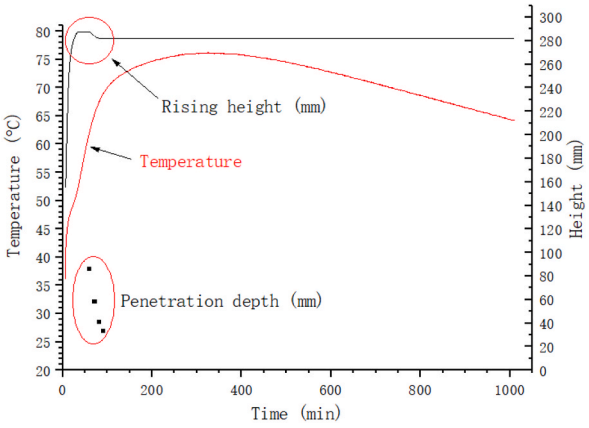

Fig. 10. Key parameters controlling the green body development: (1) rising height (h) indicates the pore structure development; (2) temperature (°C) indicates the initial hydration process; and (3) penetration depth (mm) indicates the indicator the hardening of green body.

presence of amorphous phases may negatively impact the mechanical properties and dimensional stability of AAC. Furthermore, the increased drying shrinkage of AAC with higher waste glass powder content can also contribute to the reduction in A-value at 60 % replacement.

The incorporation of waste glass powder (GP) in autoclaved aerated concrete (AAC) requires a comprehensive understanding of the interplay between the three key parameters of green body development: rising height, penetration depth, and temperature evolution (Fig. 10). By carefully considering these parameters and their relationships, it is possible to optimize the performance of AAC containing GP. The settling of the rising height should coincide with the decrease in penetration depth. This indicates that the framework between the bubbles is becoming stronger, while the gas formation is mostly complete. If the stiffening occurs too early, the increased pressure from the foaming gas may lead to the formation of cracks in the green body. Conversely, if the stiffening happens too late, there is a risk of partial collapse of the pore structure, particularly in the lower part of the green body.

Temperature plays a crucial role in balancing these processes, as an increased temperature leads to a faster reaction speed for both foaming and stiffening. The reaction heat is generated by the hydration of the lime and cement mixture, as well as the foaming reaction of the aluminum powder. While keeping these parameters constant, the thermal capacity of the ingredients changes with varying water-to-powder (W/P) ratios. Consequently, the water content becomes the limiting factor in preventing the mixture from boiling, as increased gas pressure can cause crack formation within the stiffened green body. The retarding effect of waste glass powder on the hydration of cement can help mitigate these challenges. This delay allows for a more gradual pore structure development, providing better control over the pore size distribution and interconnectivity. The slower reaction rate also helps to manage the temperature evolution, reducing the risk of boiling and crack formation.

It is important to note that the waste glass powder content has a significant impact on various aspects of AAC performance, and the optimal replacement level may depend on the specific application and desired properties. While increasing waste glass powder content can lead to improved mechanical strength, it may also result in increased shrinkage. Therefore, the selection of the appropriate waste glass powder content should be based on a careful consideration of the application requirements and a balance between the desired properties.

5. Conclusion

This study systematically investigated the incorporation of municipal waste glass powder as a partial replacement for quartz in the production of autoclaved aerated concrete, with particular emphasis on microstructure evolution, performance optimization, and industrial applicability. Through comprehensive experimental analysis and industrial-scale simulation, the following conclusions can be drawn:

1. The amorphous nature of waste glass powder alters the hydration products formation in AAC, promoting semi-crystalline calcium silicate hydrates while affecting tobermorite crystallization, thereby determining the final material properties.
2. The optimal waste glass powder replacement level is 40 %, achieving a 37 % improvement in comprehensive performance (A-value), beyond which excessive amorphous phases lead to performance deterioration.
3. The research validates the industrial feasibility of waste glass powder incorporation in AAC production, offering both environmental benefits and performance enhancement while providing practical implementation guidelines.

CRediT authorship contribution statement

C. Straub: Writing – original draft, Validation, Methodology, Investigation, Formal analysis, Data curation. **B. Yuan:** Writing –

original draft, Validation, Supervision, Resources, Project administration, Methodology, Formal analysis. **H.J.H. Brouwers:** Writing – review & editing, Resources, Project administration, Funding acquisition, Conceptualization. **W. Chen:** Writing – review & editing, Supervision, Resources, Project administration, Funding acquisition.

Declaration of Generative AI and AI-assisted technologies in the writing process

During the preparation of this work the authors used Claude in order to assist with language refinement and to enhance readability. After using this tool/service, the authors reviewed and edited the content as needed and take full responsibility for the content of the publication.

Declaration of competing interest

The authors declare that they have no known competing financial interests or personal relationships that could have appeared to influence the work reported in this paper.

Acknowledgements

This research was funded by the National Natural Science Foundation of China 52372032, 51902235), Eindhoven University of Technology and the frame work of the Research Program of the Materials innovation institute M2i (www.m2i.nl), Project Number M81.6.12478, together with the industrial partner HESS AAC Systems. Many thanks as well to Knauf Gips KG, Holcim (Deutschland) AG, Fels-Werke GmbH and HeidelbergCement Benelux for supplying materials, and Tata Steel for using their SEM, as well as to the Fachgruppe Mineralogie/Geochemie from Martin-Luther Universität Halle-Wittenberg (Germany) for the use of their XRD. Furthermore, the authors wish to express their gratitude to the sponsors of the Building Materials research group at TU Eindhoven.

Data availability

Data will be made available on request.

References

[1] R. Drochytka, E. Helanová, Development of microstructure of the fly ash aerated concrete in time, Procedia Eng. 108 (2015) 624–631, https://doi.org/10.1016/j.proeng.2015.06.189.
[2] Yuanming Song, Chuanchuan Guo, Jueshi Qian, Tian Ding, Effect of the Ca-to-Si ratio on the properties of autoclaved aerated concrete containing coal fly ash from circulating fluidized bed combustion boiler, Constr. Build. Mater. 83 (2015) 136–142, https://doi.org/10.1016/j.conbuildmat.2015.02.077.
[3] R.C. Valore Jr., Cellular concretes Part 2 physical properties, ACI J, SAVE Proc. 50 (1954) 6.
[4] V.A.R. Bernard, S.M. Renuka, S. Avudaiappan, C. Umarani, M. Amran, P. Guindos, R. Fediuk, N. Ivanovich Vatin, Performance investigation of the incorporation of ground granulated blast furnace slag with fly ash in autoclaved aerated concrete, Crystals 12 (2022) 1024, https://doi.org/10.3390/cryst12081024.
[5] Kittipong Kunchariyakun, Suwimol Asavapisit, Kwannate Sombatsompop, Properties of autoclaved aerated concrete incorporating rice husk ash as partial replacement for fine aggregate, Cem. Concr. Compos. 55 (2015) 11–16, https://doi.org/10.1016/j.cemconcomp.2014.07.021.
[6] P. Walczak, J. Małolepszy, M. Reben, P. Szymański, K. Rzepa, Utilization of waste glass in autoclaved aerated concrete, Procedia Eng. 122 (2015) 302–309, https://doi.org/10.1016/j.proeng.2015.10.040.
[7] A. Stepien, M. Leśniak, M. Sitarz, A sustainable autoclaved material made of glass sand, Buildings 9 (2019) 232, https://doi.org/10.3390/buildings9110232.
[8] André Hauser, Urs Eggenberger, Thomas Mumenthaler, Fly ash from cellulose industry as secondary raw material in autoclaved aerated concrete, Cement Concr. Res. 29 (1999) 297–302, https://doi.org/10.1016/S0008-8846(98)00207-5.
[9] Xiao-yan Huang, Wen Ni, Wei-hua Cui, Zhong-jie Wang, Li-ping Zhu, Preparation of autoclaved aerated concrete using copper tailings and blast furnace slag, Constr. Build. Mater. 27 (2012) 1–5, https://doi.org/10.1016/j.conbuildmat.2011.08.034.
[10] Yuanming Song, Baoling Li, En Hua Yang, Yiquan Liu, Tian Ding, Feasibility study on utilization of municipal solid waste incineration bottom ash as aerating agent for the production of autoclaved aerated concrete, Cem. Concr. Compos. 56 (2015) 51–58, https://doi.org/10.1016/j.cemconcomp.2014.11.006.
[11] H. Kurama, I.B. Topçu, C. Karakurt, Properties of the autoclaved aerated concrete produced from coal bottom ash, J. Mater. Process. Technol. 209 (2009) 767–773, https://doi.org/10.1016/j.jmatprotec.2008.02.044.
[12] A. Thongtha, S. Maneewan, A. Fazlizan, Enhancing thermal performance of autoclaved aerated concrete (AAC) incorporating sugar sediment waste and recycled AAC with phase change material-coated applications for sustainable energy conservation in building, Sustainability 15 (2023) 14226, https://doi.org/10.3390/su151914226.
[13] H. El-Didamony, A.A. Amer, M.S. Mohammed, M.A. El-Hakim, Fabrication and properties of autoclaved aerated concrete containing agriculture and industrial solid wastes, J. Build. Eng. 22 (2019) 528–538, https://doi.org/10.1016/j.jobe.2019.01.023.
[14] K.L. Watson, Autoclaved aerated concrete from slate waste Part 2: some property/porosity relationships, Int. J. Lightweight Concr. 2 (1980) 121–123, https://doi.org/10.1016/0262-5075(80)90014-7.
[15] S. Li, J. Zhang, G. Du, Z. Mao, Q. Ma, Z. Luo, Y. Miao, Y. Duan, Properties of concrete with waste glass after exposure to elevated temperatures, J. Build. Eng. 57 (2022) 104822.
[16] G. Liu, M.V.A. Florea, H.J.H. Brouwers, The role of recycled waste glass incorporation on the carbonation behaviour of sodium carbonate activated slag mortar, J. Clean. Prod. 292 (2021) 126050, https://doi.org/10.1016/j.jclepro.2021.126050.
[17] I. Mukangali, C.S. Shon, K. Kryzhanovskiy, D.C. Zhang, J.R. Kim, Effects of waste soda-lime glass sand and glass fiber on physical and mechanical properties of none-autoclaved aerated concrete, in: Mater. Sci. Forum, Trans Tech Publ, 2021, pp. 141–146. https://www.scientific.net/MSF.1023.141. (Accessed 24 April 2024).
[18] A. Majdinasab, Q. Yuan, Synthesis of Al-substituted 11Å tobermorite using waste glass cullet: a study on the microstructure, Mater. Chem. Phys. 250 (2020) 123069, https://doi.org/10.1016/j.matchemphys.2020.123069.
[19] G. Stanescu, A. Badanoiu, A. Nicoara, G. Voicu, Brick and glass waste valorisation in the manufacture of aerated autoclaved concrete, Rev. Chim. 70 (2019) 828–834, https://doi.org/10.37358/RC.19.3.7015.
[20] U. Avila-Lopez, J.M. Almanza-Robles, J.I. Escalante-García, Investigation of novel waste glass and limestone binders using statistical methods, Constr. Build. Mater. 82 (2015) 296–303, https://doi.org/10.1016/j.conbuildmat.2015.02.085.

[21] G. Xue, E. Yilmaz, G. Feng, S. Cao, Bending behavior and failure mode of cemented tailings backfill composites incorporating different fibers for sustainable construction, Constr. Build. Mater. 289 (2021) 123163.
[22] B. Yan, H. Jia, E. Yilmaz, X. Lai, P. Shan, C. Hou, Numerical study on microscale and macroscale strength behaviors of hardening cemented paste backfill, Constr. Build. Mater. 321 (2022) 126327, https://doi.org/10.1016/j.conbuildmat.2022.126327.
[23] G. Liu, M.V.A. Florea, H.J.H. Brouwers, The hydration and microstructure characteristics of cement pastes with high volume organic-contaminated waste glass powder, Constr. Build. Mater. 187 (2018) 1177–1189, https://doi.org/10.1016/j.conbuildmat.2018.07.162.
[24] Y. Jiang, T.-C. Ling, K.H. Mo, C. Shi, A critical review of waste glass powder – multiple roles of utilization in cement-based materials and construction products, J. Environ. Manag. 242 (2019) 440–449, https://doi.org/10.1016/j.jenvman.2019.04.098.
[25] B. Yuan, C. Straub, S. Segers, Q.L.L. Yu, H.J.H.J.H. Brouwers, Sodium carbonate activated slag as cement replacement in autoclaved aerated concrete, Ceram. Int. 43 (2017) 6039–6047, https://doi.org/10.1016/j.ceramint.2017.01.144.
[26] A. Georgiades, Ch Ftikos, J. Marinos, Effect of micropore structure on autoclaved aerated concrete shrinkage, Cement Concr. Res. 21 (1991) 655–662, https://doi.org/10.1016/0008-8846(91)90116-Y.
[27] J. Alexanderson, Relations between structure and mechanical properties of autoclaved aerated concrete, Cement Concr. Res. 9 (1979) 507–514.
[28] A. Stumm, Cement and sulphate free autoclaved aerated concrete, in: 5th Int. Conf. Autoclaved Aerated Concr. Bydg. Polen2011, 2011, pp. 375–379.
[29] H.F.W. Taylor, Cement Chemistry, second ed., Thomas Telford, 1997.
[30] I.G. Richardson, The nature of C-S-H in hardened cements, Cement Concr. Res. 29 (1999) 1131–1147, https://doi.org/10.1016/S0008-8846(99)00168-4.